Authors accepted manuscript.
Article published in IEEE Transactions on Smart Grid (Vol. 11, Issue 6, Nov. 2020)
The final published version available at https://doi.org/10.1109/TSG.2020.3002668

Crosstalk Suppression in Semi-Intrusive Load Monitoring Systems Using Hall Effect Sensors

Antoine Langevin, Ghyslain Gagnon, *Member, IEEE,* and Mohamed Cheriet, *Senior Member, IEEE*

***Abstract*—Semi-intrusive load monitoring (SILM) is an appliance load monitoring approach using multiple meters, each meter measuring power for a subgroup of appliances. As an effective solution for demand response programs, SILM is used to get granular power measurements at the level of individual appliances in buildings. Hall effect sensors (HES) on each wire attached to a circuit breaker in distribution panels are one means of providing SILM. However, HES are greatly affected by crosstalk noise generated by neighboring wires, up to 35% of interfering signals. To remove crosstalk noise, this work proposes a blind source separation (BSS) approach designed to deal with sparse matrices, making SILM measurements accurate for home energy management systems. Our approach leverages two key elements: (i) a BSS algorithm based on non-correlation for sparse mixing matrix; (ii) a sensor gain compensation that leverages smart meter readings. The results demonstrate that the total power estimation error is reduced from 15% to 2% on the *Tracebase* dataset, and from 55% to 9% on our HES dataset monitored in a family home. Furthermore, the proposed approach outperforms standard BSS algorithms such as FastICA and InfoMax. This work shows that HES can be used for load monitoring in smart buildings.**

***Index Terms*—Semi-intrusive load monitoring (SILM), Hall effect sensor (HES), blind source separation (BSS), home energy management system (HEMS)**

I. Introduction

In October 2018, the Intergovernmental Panel on Climate Change urged the reduction of 45% of greenhouse gas emissions by 2030 [1]. Some of these emissions are due to energy generation and consumption, with buildings being responsible for 20% of the global energy consumption [2]. In this scenario, smart energy management solutions are paramount to reach the reduction goal [3].

A home energy management system (HEMS) is a demand response tool helping demand side management within a smart grid [4]. It influences and optimizes household energy consumption by shifting or reducing demand load according to different criteria such as electricity price, consumer comfort, renewable energy production, or other external information [5], [6]. Based mainly on real-time and time-of-use pricing approaches, a HEMS could reduce the operational cost of electricity by 23% or residential peak demand by 30%, [6]. Furthermore, the automation of HEMS is useful to analyze the complexity of smart pricing, demand and energy production, and to plan an appropriate response, avoiding customers' intervention to manage their household devices. However, the efficiency of HEMS requires an appliance load monitoring (ALM) system to detect states and measure the power consumption of individual appliances in a home [3], [4]. From intrusive to non-intrusive solutions, many ALM techniques can be used to measure the consumption of individual household appliances [7].

Non-intrusive load monitoring (NILM) is a technique to monitor appliance load activities from a single sensor. This sensor measures the building's total consumption, and a disaggregation algorithm extracts individual consumption of each appliance. NILM is promoted as an effective ALM solution for the future. However, the complexity of the disaggregation task increases exponentially with the number of appliances and states. This constraint limits the number of appliances to approximately nine, and the performance decreases as the number of appliances increases [8]. This scalability issue and the obstacle of near real-time capabilities are only a few examples of unsolved challenges preventing NILM use in a practical context.

These challenges lead to another class of ALM, called semi-intrusive load monitoring (SILM), in which multiple sensors are used to monitor *groups* of appliances. Instead of performing the recognition task for all devices on one aggregated signal, SILM consists of several aggregated points with classifiers to recover the energy consumption of individual appliances [9]. Because of the lower number of appliances per aggregated point, SILM classifiers require a lower sampling rate and fewer features than NILM systems, which measure all appliances using only one aggregated point. It was shown in [10] that these reduced requirements lead to a lower hardware cost and decrease the computational complexity of the disaggregation task.

This paper introduces a SILM solution relying on low-cost sensors to estimate crudely the current in circuits. The proposed SILM uses Hall effect sensors (HES), which calculate the root mean square (RMS) value of the electric current flowing across a wire by measuring the magnetic field generated around it [11]. Sensors are installed on wires attached to circuit breakers in the distribution panel and communicate their I_{RMS} readings to a hub through the wired RS-485 standard, as shown in Fig. 1. The hub used in the proposed SILM system is a Raspberry Pi mounted with our custom shield compatible with the RS-485 standard. Using Wi-Fi connection, the hub communicates with a cloud server, where a disaggregation algorithm extracts the consumption of each appliance on circuits containing several appliances. Further analysis on appliance activities can be achieved in the cloud and shared with the HEMS to make informed decisions

A. Langevin, and M. Cheriet are with Synchromedia Laboratory - École de technologie supérieure, Université du Québec (Canada).
E-mail: antoine.langevin.1@etsmtl.net

G. Gagnon is with LaCIME Laboratory - École de technologie supérieure, Université du Québec (Canada).

on energy conservation and load management. However, HES are affected by any magnetic field in their vicinity. This notwithstanding, two main impediments to the widespread use of this SILM are (1) HES are affected by crosstalk noise created by neighboring circuits in the distribution panel, and (2) the sensors' sensitivity varies depending on their physical positions during the installation. As much as 35% of another signal can be seen as crosstalk noise on sensor measurements. Over time, this noise creates a shift between the measured and real energy consumption, generating errors in the estimation.

Since noisy sensor measurements correspond to the sum of multiple circuits' power consumption, the crosstalk noise can be formulated as a blind source separation (BSS) problem. However, standard BSS algorithms fail this particular signal separation task because of the sparsity of the mixing matrix. Usually, only four or five of the closest circuits generate crosstalk noise on sensor measurements in a system that typically contain more than 15 circuits, causing a sparse mixing matrix. The second issue encountered with HES is the variability of the sensor gain created by the high sensitivity of these sensors: the position of the sensor on the circuit breaker wire can generate measurement variations of more than 20% depending on the angle of the sensor during the installation. Crosstalk gains and sensor gains stay constant as long as there is no movement in the distribution panel.

The aim of this paper is to propose a low-cost SILM solution based on HES. In order to obtain accurate measurements, the crosstalk noise generated by neighboring circuits has to be removed, and the HES sensor gain must be auto-calibrated. The contributions of this research are as follows:

- A BSS approach based on a deterministic non-correlation solution is proposed to remove crosstalk noise in sensor measurements. Our approach handles classes of problems which are challenging for BSS algorithms, i.e. problems with either sparse mixing matrices, low mixing coefficients or imbalanced signal levels.
- A sensor gain compensation based on an adaptive filter leveraging smart meter readings is proposed to adjust HES measurement levels.
- A new power consumption dataset monitored with the proposed HES-based SILM system in a family home is used to compare our approach with standard BSS algorithms. This dataset also introduces new empirical data to help benchmark future SILM and NILM systems and is available publicly.[1]

The rest of this paper is organized as follows. Section II gives a brief overview of ALM and BSS techniques, followed by the formulation of the HES crosstalk noise problem in Section III. The proposed solution for the sparse mixing matrix BSS approach is presented in Section IV. Section V describes experiments done on simulated and real environments, followed by results and discussions for each of them. Finally, the paper concludes and projects future research in Section VI.

[1]https://github.com/ETSSmartRes/HES-Dataset

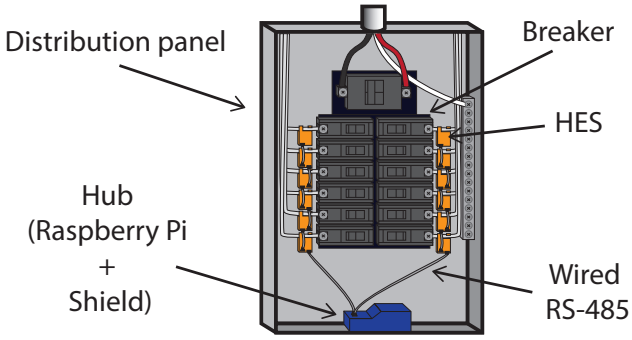

Fig. 1. The proposed SILM system using HES installed in a distribution panel

II. Related Work

This section reviews ALM techniques for intrusive and non-intrusive systems. Furthermore, a brief literature review describes the SOS and HOS techniques used as benchmark algorithms in Section V.

A. ALM Techniques

Throughout the literature, many ALM techniques have been proposed. A straightforward method to monitor individual household appliances is intrusive load monitoring, which is obtained by deploying a power meter on each appliance in a building. These sensors are broadly current transformers (CT) or, more recently, smart plugs. Although highly accurate, this approach has high installation and operation costs [12], and recessed appliances cannot be monitored [13]. Moreover, there are privacy concerns around this technique, which prevent large-scale acceptance of this technology [14]. These drawbacks have led to the introduction of NILM techniques.

NILM approaches, first proposed by Hart [15], utilize one sensor that monitors the whole house's electric consumption, and a disaggregation algorithm identifies and extracts the power of individual appliances [13]. NILM methods are generally categorized into two groups: state-based methods and event-based methods. State-based methods focus on detecting the active states of each appliance. These approaches use steady-state features such as edge measurements when an appliance turns ON/OFF or changes its running states. Monitored signals include active power, reactive power, current and voltage waveforms. These signals are typically obtained at a low sampling rate, less than 1 Hz, reducing the hardware cost and allowing the use of smart meter measurements. State-based algorithms are usually based on a hidden Markov model and its variants [16], [17]. He et al. [18] also propose a graph signal processing algorithm for energy disaggregation. These state-based methods generally achieve better performance, especially with ON/OFF and finite state appliances, but struggle to monitor variable and continuous appliances [19]. More recently, [20], [21] have proposed approaches for NILM based on deep neural networks, such as Long-Short Term Memory and denoising autoencoders. However, these models need supervised training, which is time-consuming and requires sub-metering during the training process. Furthermore, the deployment performance is sensitive to the training dataset, making unseen buildings harder to monitor [19].

On the other hand, event-based approaches characterize signal edges when a state change occurs. These approaches use transient features that require a higher sampling rate, in the kHz range or more, demanding more expensive hardware. By characterizing the transition signals, these methods can classify the signal edges and associate the power to a specific appliance, which is starting or changing state. This category of methods is based on features such as shape, size, duration, and harmonics of current or power waveforms [19]. Methods used to classify transient features are primarily machine learning classifiers such as support vector machine and neural networks [22], [23]. A voltage-current trajectory is also used in [12] for feature extraction.

Most NILM performances are highly affected by the increasing number of appliances in the aggregate signal [9], [10], [17]. This problem contributed to the development of SILM, which minimizes the number of sensors, thus balancing installation cost and performance.

B. BSS Techniques

BSS is a known problem in the telecommunications, biomedical, audio, and other fields [24], where the objective is to recover source signals using only mixture observations. Static or instantaneous mixing is the most typical model seen in the BSS domain and is characterized by matrix multiplication. The problem described in this paper is considered a *determined* mixture with an equal number of observations M and sources N. Second-order statistics (SOS) and higher-order statistics (HOS) are the two main categories of methods to solve determined BSS problems. Algorithms based on SOS, such as principal component analysis (PCA) [25], AMUSE [26], SOBI [27], and WASOBI [28] work well when sources are Gaussian and assumed to be stationary. Thus, for non-Gaussian distribution signals, HOS are more suitable to remove the crosstalk noise on HES. To validate this, we performed experiments on several SOS algorithms. The PCA algorithm provided the best results and was thus chosen as the SOS comparative algorithm in Section V.

Independent component analysis (ICA) [29]–[33], the most popular group of HOS algorithms is mainly used to do BSS, but also for feature reduction in machine learning, localization of sources, compression, and more. ICA's objective is to find independent components from mixture signals using different methods. Mutual information minimization, maximum likelihood estimation, non-Gaussianity maximization, or a combination of these are some techniques used to maximize independence between signals. Two assumptions are made to use ICA algorithms. First, the number of observations M is equal to the number of sources N and, secondly, at most, only one signal can be Gaussian.

FastICA [30] with non-Gaussianity optimization searches for the optimal unmixing matrix that maximize the Gaussian distance between signals. This is achieved by minimizing nonlinear functions, such as kurtosis. The FastICA algorithm converges fast and is an efficient separation algorithm. Other variations of non-Gaussianity approaches have been developed using non-parametric score functions, such as RADICAL [32] and NPICA [33]. These two methods get accurate separation results, but they are computationally complex. Furthermore, they have difficulty in separating more than ten signals in practice, which is a drawback for HES networks, where the number of signals is typically larger than 15 in standard houses [34].

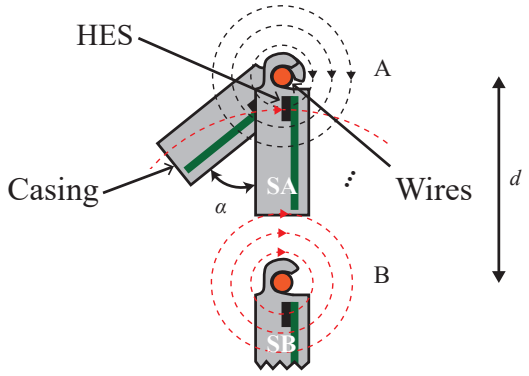

Fig. 2. Schematic description of the magnetic field generated by wire **B** creating crosstalk noise on the sensor **SA**

InfoMax [31] is another popular ICA algorithm that minimizes mutual information between the outputs, but the nonlinear function used is a logistic sigmoid more adapted for real-world signals having a super-Gaussian probability density function.

Nonnegative matrix factorization (NMF) [35] is a BSS algorithm based on non-negativity constraint which achieves meaningful representation in many domains. However, NMF is well suited for problems with a number of sources superior to the number of observations, making this algorithm useful in the context of undetermined problems, such as hyperspectral data processing, image analysis, sparse coding, etc. For the crosstalk noise suppression task in HES measurements, the NMF algorithm did not achieve good results.

Generalized Morphological Component Analysis (GMCA) [36] and Adaptive Morphological Component Analysis (AMCA) [37] are more recent BSS algorithms, which are especially suitable for images source separation problems. Even though these algorithms can be adapted to time series, they did not work with many observations over long time series. Furthermore, the execution time was typically $\sim$200 times longer than ICA algorithms.

In this work, we opted for the PCA, FastICA and InfoMax approaches to be used as comparative algorithms for the proposed solution described in Section IV.

III. Problem Formulation

The proposed SILM uses HES to estimate the RMS current by measuring the magnetic field generated around wires. As these sensors are also affected by magnetic fields generated by other circuits in the distribution panel, the measurement accuracy is thus reduced because of crosstalk noise.

As shown in Fig. 2, various parameters affect the level of crosstalk noise generated on sensors. In this example, the distance d separating the two wires and the angle α influence the noise level generated by wire **B** on sensor **SA**. Another issue is the variability of sensor sensitivity, referred to as sensor gain in this paper. A slight variation of the sensor position during the installation affects its sensor gain. The

crosstalk noise can be observed on single and multiple phases electrical distribution.

The HES monitoring issue is defined as a BSS problem, since the noisy sensor measurements correspond to the sum of multiple circuits. This BSS problem can be characterized as a linear mixture and a determined system in which the number of circuits (sources) M and the number of sensors (observations) N are equal. Using the conventional BSS notation [38], the HES monitoring problem is described as

$$\mathbf{x}(t) = \mathbf{A}\mathbf{s}(t), \tag{1}$$

where $\mathbf{x}(t)$ is the sensor measurements vector of dimension N in time domain $t \in \{0, \ldots, T\}$ comprising instantaneous mixtures, i.e., measurements plus crosstalk noise from other circuits; $\mathbf{A}$ is the mixing matrix of dimension $N \times N$ describing the physical phenomenon of crosstalk noise; and $\mathbf{s}(t)$ is the vector of dimension N in time domain t corresponding to the real current flowing in circuits.

The classical BSS example is the cocktail party problem: multiple conversations occurring simultaneously in a room. A series of microphones record sounds, $\mathbf{x}(t)$, in that room, but the recordings contain a mixture of every conversation. Thus, the objective is to estimate $\hat{\mathbf{A}}$ in order to restore the original conversations, $\mathbf{y}(t)$, as given by,

$$\mathbf{y}(t) = \hat{\mathbf{A}}^{-1}\mathbf{x}(t). \tag{2}$$

If $\hat{\mathbf{A}}$ is correctly estimated, the vector $\mathbf{y}(t)$ is equal to $\mathbf{s}(t)$.

Translated into the current problem, the mixing matrix $\mathbf{A}$ reflects the exact issues of the HES-based SILM. The diagonal of matrix $\mathbf{A}$ corresponds to the sensor gains, whereas other coefficients correspond to the proportion of crosstalk noise generated by other circuits. The objective of the proposed solution is to remove the crosstalk noise and to adjust sensor gains by estimating matrix $\hat{\mathbf{A}}$ so that $\mathbf{y}(t)$ corresponds to the real circuit currents.

IV. Proposed Solution

The overall process to estimate the sparse mixing matrix $\hat{\mathbf{A}}$ is described in Fig. 3. The main steps of the proposed solution are as follows:

1) Identification of high-activity segments (HAS) based on a thresholding method to detect high power variations on HES measurements and to reduce dimensionality;
2) Creation of a pairing matrix based on correlation between HES measurements to identify sensors affected by crosstalk noise;
3) Crosstalk noise suppression using non-correlation evaluation on noisy sensors identified by the pairing matrix;
4) Sensor gain compensation leveraging smart meter readings based on the least mean square (LMS) algorithm [39].

A. HAS Detection Process (Step 1)

As the first step of the crosstalk gain estimation, the HAS detection process is developed as a tool used by the creation of the pairing matrix (step 2), and the crosstalk noise suppression (step 3), both based on the correlation between the measurements of all of the sensors. Thus, the objective of this first step is to identify a maximum of segments in which high electrical activities occur on signal measurements over period T.

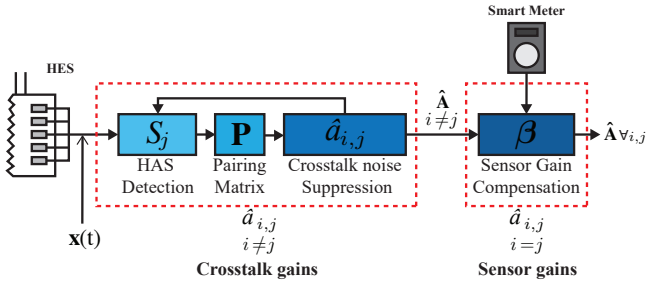

Fig. 3. Overall flow of the proposed solution to estimate crosstalk and sensor gains

In general, power consumption by appliances has a marked variation when appliances are changing state. Therefore, as in the NILM algorithm in [18], which uses variations in power measurements to detect appliances' changing states, we opted for a threshold strategy to identify high electrical variations. Using the first derivative of sensor measurement, we identify all times τ where the derivative is higher than δ. The optimal threshold value, δ, found through a grid search technique on a validation dataset during training, corresponds to 0.3A. For each τ, the algorithm verifies if a higher variation occurs on another sensor to ensure that the variation detected corresponds to the monitored circuit.

For an HAS detected at time $t = \tau$, we collect the samples of all sensors for that segment in:

$$\mathbf{h} = \big[\mathbf{x}(\tau - d), \ldots, \mathbf{x}(\tau), \ldots, \mathbf{x}(\tau + d)\big], \tag{3}$$

where, the HAS length is $M = 2d + 1$, and $\mathbf{x}(t)$ is the measurement vector of all sensors at time t. This algorithm is executed on the entire length of the dataset, leading to many detections of HAS. These segments are grouped in the ensemble H_i for each sensor i:

$$H_i = \big\{\mathbf{h}^1, \ldots, \mathbf{h}^k, \ldots, \mathbf{h}^{K_i}\big\}, \tag{4}$$

where K_i is the number of segments detected. This HAS detection process is then executed for each sensor.

B. Pairing Matrix Creation (Step 2)

As a second step for the crosstalk noise suppression, the correlation value between sensors' measurements is calculated to obtain the pairing matrix, $\mathbf{P}$. Crosstalk noise affects mostly neighboring circuits, creating a sparse mixing matrix. Therefore, the pairing matrix aims to reduce the number of coefficients, $\hat{a}$, to estimate, considering that the total number equals N^2. Using the pairing matrix, crosstalk gains $\hat{a}_{i,j}$ are only calculated (step 3) when the pairing value, $p_{i,j}$, is higher than threshold θ.

In order to obtain $\mathbf{P}$, we use all HAS from the previous step to calculate the correlation value between sensors i and j:

$$\hat{r} = \frac{\hat{\sigma}_{\mathbf{h}_i\mathbf{h}_j}}{\hat{\sigma}_{\mathbf{h}_i}\hat{\sigma}_{\mathbf{h}_j}}, \tag{5}$$

where $\hat{\sigma}_{\mathbf{h}_i\mathbf{h}_j}$ is the covariance; and $\hat{\sigma}_{\mathbf{h}_i}$ and $\hat{\sigma}_{\mathbf{h}_j}$ are the standard deviation for sensors i and j respectively.

The correlation value is calculated between sensor i and the other sensors using all segments $\mathbf{h} \in H_i$. The averaged correlation over all HAS is then calculated and inserted in matrix $\mathbf{P}$ at row j and column i. The same steps are repeated for each sensor to complete the pairing matrix.

C. Crosstalk Noise Suppression (Step 3)

All circuits are assumed to be independent in such a way that the non-correlation evaluation can be done individually between each sensor for which the pairing matrix, $\mathbf{P}$, detected crosstalk noise, $p_{i,j} > \theta$. According to the training on a validation dataset using a grid search technique, crosstalk noise is detected optimally when $p_{i,j}$ is higher than threshold $\theta = 0.2$.

First, let us define:

$$\mathbf{w}_i = \mathbf{x}_i - \hat{a}_{i,j} \cdot \mathbf{x}_j \text{ when } i \neq j \text{ and } p_{i,j} > \theta, \tag{6}$$

where $\mathbf{w}_i$ is the cleaned signal measurement of sensor i when the crosstalk generated by the circuit j is subtracted. Here, $\mathbf{x}_i$ is the sensor measurement of circuit i affected by crosstalk noise generated by circuit j; $\mathbf{x}_j$ is the sensor measurements of the circuit causing noise; and $\hat{a}_{i,j}$ corresponds to the estimated proportion of $\mathbf{x}_j$ appearing in $\mathbf{x}_i$.

Using (5), the correlation value between $\mathbf{x}_j$ and $\mathbf{w}_i$ is zero when the estimated coefficient $\hat{a}_{i,j} = a_{i,j}$ and the crosstalk noise from $\mathbf{x}_j$ is completely subtracted of $\mathbf{x}_i$. The objective is to find $\hat{a}_{i,j}$ so that the correlation between $\mathbf{x}_j$ and $\mathbf{y}_i$ is null. Using H_j from the HAS detection process (step 1), the estimated proportion $\hat{a}_{i,j}$ for one HAS is given by the following equation:

$$\hat{a}_{i,j} = \frac{(M\mathbf{h}_j - \mathbf{h}_j\mathbf{J})(\mathbf{h}_i\mathbf{J} - M\mathbf{h}_i)^{\mathbf{T}}}{(M\mathbf{h}_j - \mathbf{h}_j\mathbf{J})(\mathbf{h}_j\mathbf{J} - M\mathbf{h}_j)^{\mathbf{T}}}, \tag{7}$$

where,
$\mathbf{h}_i$ and $\mathbf{h}_j$ are segments of sensors measurements i and j respectively;
$\mathbf{J}$ is an all-ones column vector of dimension $M \times 1$;
$(\cdot)^{\mathbf{T}}$ denotes the transpose operation.

Equation (7) is used to estimate $\overline{a}_{i,j}$, taking the average over all $\mathbf{h} \in H_j$ corresponding to all the HAS of the sensor causing noise.

The estimation of each averaged $\overline{a}_{i,j}$ is done sequentially and is calculated following a descending order from the sensor with the highest power measurement to the sensor with the lowest power measurement. In this way, sensors with more noise than real power will be cleaned of their noise first so that a better estimated real power can be used when identifying HAS in further steps. Furthermore, outliers, $\hat{a}_{i,j}$, outside the range $[0, 1]$ are removed from averaged calculations. Algorithm 1 summarizes the steps to estimate coefficients of mixing matrix $\hat{\mathbf{A}}$.

D. Sensor Gain Compensation (Step 4)

After completion of step 3, the estimated mixing matrix $\hat{\mathbf{A}}$ has been optimized for all $i \neq j$. However, sensor gains, diagonal values of $\hat{\mathbf{A}}$, are still at the initial value of one. A reliable reference is needed to estimate sensor gains. We opted for smart meter readings as a reference value for the adaptive filter in the last step of the proposed solution.

Algorithm 1 Crosstalk Gains Estimation Based on Non-correlation Evaluation

Set $\hat{\mathbf{A}} = \mathbf{I}$
for all sensors **do**
  $\hat{\mathbf{y}}(t) = \hat{\mathbf{A}}^{-1}\mathbf{x}(t)$
  Select the sensor with the highest power consumption
  $j = \text{argmax}_j\, \hat{\mathbf{y}}(t)$
  $H_j \Leftarrow$ Extracted HAS for sensor j
  $\mathbf{P} \Leftarrow$ Creating the pairing matrix
  for all sensors $i \neq j$ so that $p_{i,j} > \theta$ **do**
    for all h in H_j **do**
      $\mathbf{x}_j = \mathbf{h}_j$
      $\mathbf{w}_i = \mathbf{h}_i - \hat{a}_{i,j} \cdot \mathbf{h}_j$
      Non-correlation evaluation (7)
      $\hat{a}_{i,j} \in \frac{\hat{\sigma}_{\mathbf{x}_j\mathbf{w}_i}}{\hat{\sigma}_{\mathbf{x}_j}\hat{\sigma}_{\mathbf{w}_i}} = 0$ s.t. $0 < \hat{a}_{i,j} < 1$
    end for
    $\overline{a}_{i,j} = \text{mean}(\hat{a}_{i,j})$
    Update $\hat{\mathbf{A}}$
    $\hat{\mathbf{A}}_{i,j} \leftarrow \overline{a}_{i,j}$
  end for
end for

The LMS adaptive filter used in [40] is an iterative algorithm requiring only instantaneous values. The LMS recursive iteration is given by,

$$\boldsymbol{\beta}_n = \boldsymbol{\beta}_{n-1} + \mu \cdot \mathbf{y}(n) \cdot \left[d(n) - \mathbf{y}^{\mathbf{T}}(n) \cdot \boldsymbol{\beta}_{n-1}\right], \tag{8}$$

where $\boldsymbol{\beta}_n$ is the sensor gain column vector estimated at the nth iteration; μ is a positive step-size; and $\mathbf{y}(n)$ and $d(n)$ are denoised sensors measurement and smart meter measurement.

All elements of $\boldsymbol{\beta}_0$ are initialized to one, and we iterate (8) over all data $\mathbf{x}(t)$ available until convergence of each sensor gain. Then the column vector $\boldsymbol{\beta}$ is transformed into a diagonal matrix, and the cross product is performed with $\hat{\mathbf{A}}$ from step 3, to find the final mixing matrix $\hat{\mathbf{A}}$.

Finally, the corrected signal $\mathbf{y}(t)$ can be calculated with the estimated $\hat{\mathbf{A}}$ and the mixed signals $\mathbf{x}(t)$ using (2).

V. Case Study

Two case studies were performed to evaluate the proposed crosstalk noise suppression algorithm, and the sensor gain compensation of the proposed HES-based SILM system. The first case study uses the *Tracebase* dataset to compare performances of our approach with two BSS algorithms on three specific configurations. The second case study tests the proposed approach on our HES dataset created from a family home containing more sensors.

A. Performance Metrics

Most household electrical appliances have imbalanced classes, with many more OFF states, preventing the use of the accuracy metric. In order to evaluate case study performance, the following metrics from NILM research are used [8]:

1) F-Measure (F_m): For each sensor in the system, a class is assigned for all points in time $t = 1$ to T. To perform the class assignment, each power measurement is compared to a threshold; if the power exceeds this threshold, the appliance is assigned to the class ON, otherwise, the appliance is assigned to the class OFF. The metric used to evaluate state assignment performance is given by,

$$F_m = \frac{2 \cdot PR \cdot RE}{(PR + RE)}, \tag{9}$$

where PR and RE are precision and recall respectively.

2) Estimation Error (η): To evaluate individual sensor performance, the estimation error based on the ratio of the estimated power on the real power is defined as follows:

$$\eta = \left| \frac{\sum_{t=1}^{T} \hat{y}_i(t) - y_i(t)}{\sum_{t=1}^{T} y_i(t)} \right| \cdot 100\%, \tag{10}$$

where $\hat{y}_i(t)$ and $y_i(t)$ are the estimated and the real measurement of sensor i at time t, respectively. The estimation error gives an understanding of the monitoring accuracy per appliance and is an indicator of individual crosstalk noise suppression performance.

3) Total Power Estimation Error (η_{tot}): To assess the total power estimation error of the whole SILM system, this metric calculates the total error for all sensors divided by the real aggregate power. The total power estimation error is given by

$$\eta_{tot} = \frac{\sum_{t=1}^{T} \sum_{i=1}^{N} \left| \hat{y}_i(t) - y_i(t) \right|}{\sum_{t=1}^{T} \sum_{i=1}^{N} y_i(t)} \cdot 100\%. \tag{11}$$

B. Post-Processing for Comparative BSS Algorithms

One issue in using ICA algorithms to remove crosstalk noise in HES measurements is that the resulting outputs of these algorithms return the estimated sources, but scale, sign, and order are not preserved; but the latter are critically important for this application. In order to be able to compare the proposed algorithm with PCA, FastICA and InfoMax, a post-processing algorithm was used to adjust the estimated mixing matrix $\hat{\mathbf{A}}$.

C. Case Study 1

The first case study was performed to evaluate the proposed crosstalk noise suppression approach and to compare it with three standard BSS algorithms. Three configurations were tested with different levels of crosstalk noise using real appliances' power consumption signals from the *Tracebase* [41] dataset.

1) Procedure: With more than 40 appliances, the public dataset *Tracebase* was used to create custom sets of appliance consumption. Ten typical household appliances were chosen. In order to evaluate the crosstalk suppression algorithm, crosstalk noise needed to be generated on each sensor's measurements. It was simulated by adding the consumption measurements of two other appliances. The mixing matrix was generated randomly, and $\mathbf{x}(t)$ was calculated using (1). Previous experiments have shown that crosstalk gains and sensor gains follow an exponential distribution and a normal distribution, respectively. To reduce bias, one hundred independent experiments with a random mixing matrix were performed for each configuration.

Config.	Sensor Gain Range	Crosstalk Gain Range
1	$a_{i,i} \sim \mathcal{N}(1, 0.05)$	$a_{i,j} \sim Exp\,(40)$
2		$a_{i,j} \sim Exp\,(15)$
3		$a_{i,j} \sim Exp\,(8)$

TABLE I
COEFFICIENT RANGES FOR EACH CONFIGURATION

Table I shows coefficient ranges for both sensor and crosstalk gains for three configurations. Configuration 2 corresponds to the most realistic scenario as per our previous experiments performed with HES sensors in our laboratory, with sensor gains varying $\pm$ 15% and crosstalk noise up to 39%.

For each experiment, the four steps of the proposed approach described in Section IV were performed to estimate the mixing matrix $\hat{\mathbf{A}}$. The aggregate consumption used by the LMS algorithm was simulated by summing all appliance measurements and downsampled to 30 minutes. In order to compare the proposed solution with standard BSS algorithms, PCA, FastICA and InfoMax were used to estimate the mixing matrix and remove the crosstalk noise. The same LMS algorithm described in IV-D was used to adjust sensor gains for these comparative algorithms.

The procedure for each configuration was divided into three steps, as described below:

1) Generate data for the experiment
   a) Randomly select appliances to generate crosstalk noise to other sensors
   b) Randomly generate the mixing matrix $\mathbf{A}$ for a specific configuration
   c) Generate mixed data $\mathbf{x}(t)$ using (1)
2) Mixing matrix coefficients estimation
   a) Estimate crosstalk gains $\hat{a}_{i,j}\ \forall\ i \neq j$
   b) Estimate sensor gains $\hat{a}_{i,j}\ \forall\ i = j$
   c) Calculate $\mathbf{y}(t)$ with the estimated mixing matrix $\hat{\mathbf{A}}$ using (2)
3) Iterate steps 1 and 2 to generate 100 independent experiments

2) Results and Discussion: Table II shows the averaged results (F_m, η) for each appliance in the 100 experiments. The mean and the standard deviation results for the whole system are in the last two columns. For each metric, the table shows the noisy signal score, i.e., measurements with the crosstalk noise, as well as, measurements with the crosstalk noise removed by the comparative algorithms (PCA; FastICA; InfoMax) and the proposed solution. The results in Table II correspond to configuration 2, whereas the results in Fig. 4 correspond to the total power estimation errors for each configuration.

As shown in Table II, the proposed BSS approach designed for the sparse mixing matrix was able to reduce the mean estimation error from 15% to 2% on simulated experiments. Individually, most of the appliances tested obtained better

Metrics		Appliances	1	2	3	4	5	6	7	8	9	10	Mean	Std
	F_m (%)	Noisy	95.3	87.0	94.1	94.6	93.5	88.2	96.3	91.2	91.8	91.4	**92.3**	3.2
		PCA	92.1	88.3	84.2	78.9	82.9	75.1	81.6	78.0	83.4	94.8	**83.9**	5.2
		FastICA	95.9	96.1	97.6	89.4	86.5	95.2	93.2	96.7	91.6	41.7	**88.4**	3.8
		InfoMax	99.0	97.1	98.1	94.0	98.8	98.3	91.1	98.4	97.8	45.5	**91.8**	2.7
		Proposed	99.9	98.3	99.1	99.0	99.6	98.6	98.9	98.6	98.8	98.3	**98.9**	0.5
	η (%)	Noisy	8.7	30.7	11.8	10.8	12.3	27.2	7.1	18.6	17.4	19.0	**16.4**	8.2
		PCA	10.5	20.8	29.6	29.3	37.9	50.9	29.7	35.0	36.3	6.3	**28.6**	11.3
		FastICA	4.9	7.4	2.5	13.4	25.2	7.9	14.7	3.3	12.8	73.2	**16.5**	7.2
		InfoMax	1.4	5.9	1.9	10.1	1.6	3.4	19.6	3.2	1.8	70.6	**11.9**	6.0
		Proposed	0.2	3.4	1.7	2.0	0.7	2.7	2.3	2.8	2.1	3.3	**2.1**	1.0

TABLE II
RESULTS OF THE 100 EXPERIMENTS AVERAGE SCORE FOR 10 APPLIANCES FROM THE *Tracebase* DATASET OF CONFIGURATION 2.
F_m: HIGHER IS BETTER AND η, η_{tot}: LOWER IS BETTER

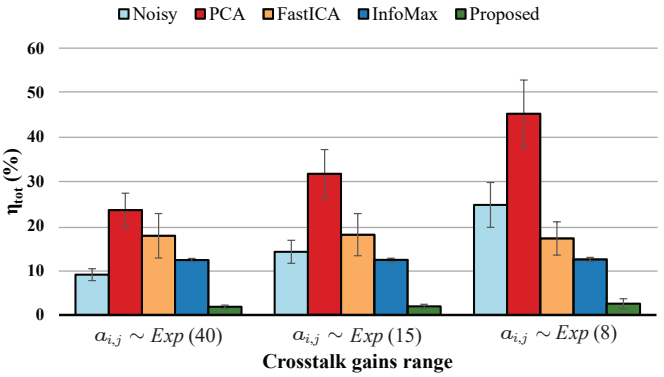

Fig. 4. Crosstalk noise suppression results for each configuration of Table I on the *Tracebase* dataset

noise reduction with the proposed BSS approach than all comparative algorithms. The crosstalk noise suppression by FastICA and InfoMax was less efficient for appliances consuming less power, e.g., appliance 10. This issue increased the individual estimation error by four times, on average, over 100 experiments. Indeed, the diversity of appliances in buildings is such that power measurements between signals are imbalanced, and the crosstalk noise is higher than the real consumption for appliance consuming low power, which makes it difficult to distinguish noise from the real consumption. The proposed approach avoids this imbalance problem by removing noise iteratively in descending order. Moreover, all BSS algorithms had problems with sparse mixing matrices. In essence, many false positive coefficients appear in the mixing matrix where there is no crosstalk noise between signals, generating additional noise in measurements. In the proposed approach, the pairing matrix step helps in that matter by identifying crosstalk noise sources before proceeding with crosstalk gain evaluation. The LMS algorithm converged on average during the first two weeks of data for a smart meter sampling period of 30 minutes. However, power activities had to be present for each sensor to adjust sensor gains adequately. In some cases, sensors with fewer electrical activities took longer to converge, but the effect was negligible over the whole house consumption.

As shown in Fig. 4, the proposed algorithm is only slightly affected by the level of crosstalk noise. The total power estimation error is almost constant between all ranges of crosstalk noise. Since each crosstalk coefficient is analyzed and optimized separately, the proposed solution is more accurate regardless of the level of crosstalk generated on signals, while FastICA and InfoMax optimize all coefficients of the unmixing matrix at the same time. On the other hand, the residual error of the PCA algorithm is proportional to the level of crosstalk noise and exhibited the poorest overall performance.

One issue affecting the accuracy of the estimated crosstalk gains for our approach occurs when the original signal varies at the same time as crosstalk noise is present in an HAS. However, this problem was minimized by using the average coefficient over all HAS and by reducing the segment length, M. Furthermore, in selecting a low threshold, θ, the pairing matrix was maximizing recall, thus detecting all pairs of sensors containing crosstalk noise. Finally, selecting a threshold δ around $0.3A$ avoids detection of variations that are too small, but allows HAS detections of appliances consuming less power.

D. Case Study 2

The second case study was performed to validate the proposed approach on our dataset created with our developed HES installed in the distribution panel of a family house.

1) Procedure: Our proposed HES-based SILM system was installed in the distribution panel of a family house to measure the current of each circuit. A total of 39 sensors were deployed to monitor the consumption of the entire house. A family of four people was living in this detached home in the region of Montreal, Canada, during the monitoring period. The period covered was May to September 2018, with a sampling rate of 1 Hz. Original measurements contain crosstalk noise from the nearest wires in the distribution panel. Since crosstalk noise generated by magnetic fields decreases proportionally with the distance between circuit wires and sensors, the number of circuits creating crosstalk noise corresponds on average to five in the HES dataset, which creates a sparse mixing matrix. The highest crosstalk gain in these measurements corresponds to 35%; the car charger circuit generating noise on the dishwasher sensor. A cleaned version of the dataset is also available in which crosstalk noise was removed manually to evaluate the performance of the proposed approach. For this empirical benchmark, sensor gains were calculated during preliminary tests and during the installation. The aggregate measurements for sensor gain compensation were then simulated using these preliminary gain values. In order to compare

Model	F_m (%)	η (%)	η_{tot} (%)
Noisy	62.6	345.3	55.8
PCA	61.8	102.3	39.3
FastICA	71.8	76.5	68.5
InfoMax	71.3	88.5	70.9
Proposed	**87.8**	**23.2**	**9.5**

TABLE III
CROSSTALK NOISE SUPPRESSION RESULTS ON THE REAL HOME DATASET

the proposed solution, all standard BSS algorithms, PCA, FastICA and InfoMax, were used to remove crosstalk noise.

2) Results and Discussion: Table III summarizes this case study's results of crosstalk suppression on the HES dataset. The proposed solution shows a significant improvement whereby the F-Measure increased by more than 25%, and the total power estimation error was reduced from 55% to 9%. The PCA algorithm performed comparatively better using the HES dataset than the previous case study, due in part to more imbalanced appliances. FastICA and InfoMax improve over PCA, but the performance of the total power estimation was worse for the cleaned signals than noisy signals. As in case study 1, the mixing matrices found by standard BSS algorithms were not sparse and some low power circuits had a higher estimation error. Our proposed solution avoids these false positive errors through the pairing matrix constraint. Some false positive errors were likewise present in the estimated mixing matrix of the proposed algorithm, but the gains associated with them were in the range of 0.005, which represents a negligible impact on performance.

VI. CONCLUSION AND FUTURE RESEARCH DIRECTIONS

The HES-based SILM presented in this work is an alternative to NILM solutions when the number of appliances in a system increases. We propose a BSS approach to remove crosstalk noise in HES measurements, mainly caused by the high density of wires in the distribution panel. Moreover, a pairing algorithm is proposed to identify sources of noise between sensors; it reduces considerably the number of mixing coefficients to be estimated in the sparse mixing matrix. Although sensor gains have a much lower influence on circuit consumption estimation errors, we propose a method to estimate them by using an LMS algorithm that leverages smart meter readings with a sampling period of 30 minutes.

The BSS approach proposed in this work could be generalized for other domains where there is crosstalk noise, such as surface electroencephalogram signals in the biomedical domain and especially when the mixing matrix is sparse. In future research involving a HES-based SILM system, we plan to reduce the number of sensors required. By leveraging the crosstalk noise present in sensor measurements, the power consumption of neighboring circuits can be monitored. This BSS problem will be more challenging to solve because the number of sensors N will be lower than the number of observations M. However, we will investigate this problem using underdetermined mixture solutions.

ACKNOWLEDGMENT

This work was supported by the Natural Sciences and Engineering Research Council of Canada (NSERC) and the Canada Research Chair (CRC).

REFERENCES

[1] IPCC, *Global warming of 1.5C. An IPCC Special Report on the impacts of global warming of 1.5C above pre-industrial levels and related global greenhouse gas emission pathways, in the context of strengthening the global response to the threat of climate change, sustainable development, and efforts to eradicate poverty*. [V. Masson-Delmotte, P. Zhai, H. O. Prtner, D. Roberts, J. Skea, P.R. Shukla, A. Pirani, W. Moufouma-Okia, C. Pan, R. Pidcock, S. Connors, J. B. R. Matthews, Y. Chen, X. Zhou, M. I. Gomis, E. Lonnoy, T. Maycock, M. Tignor, T. Waterfield (eds.).] In Press.

[2] U. EIA, "Energy information administration. international energy outlook 2016 with projections to 2040," DOE/EIA-0484, Tech. Rep., 2016.

[3] S. S. Hosseini, K. Agbossou, S. Kelouwani, and A. Cardenas, "Non-intrusive load monitoring through home energy management systems: A comprehensive review," *Renewable and Sustainable Energy Reviews*, vol. 79, pp. 1266–1274, 2017.

[4] S. Welikala, C. Dinesh, M. P. B. Ekanayake, R. I. Godaliyadda, and J. Ekanayake, "Incorporating appliance usage patterns for non-intrusive load monitoring and load forecasting," *IEEE Transactions on Smart Grid*, vol. 10, no. 1, pp. 448–461, 2019.

[5] N. Javaid, I. Khan, M. Ullah, A. Mahmood, and M. U. Farooq, "A survey of home energy management systems in future smart grid communications," in *2013 eighth international conference on broadband and wireless computing, communication and applications*. IEEE, 2013, pp. 459–464.

[6] M. Beaudin and H. Zareipour, "Home energy management systems: A review of modelling and complexity," *Renewable and sustainable energy reviews*, vol. 45, pp. 318–335, 2015.

[7] J. R. Herrero, Á. L. Murciego, A. L. Barriuso, D. H. de La Iglesia, G. V. González, J. M. C. Rodríguez, and R. Carreira, "Non intrusive load monitoring (nilm): A state of the art," in *International Conference on Practical Applications of Agents and Multi-Agent Systems*. Springer, 2017, pp. 125–138.

[8] C. Nalmpantis and D. Vrakas, "Machine learning approaches for non-intrusive load monitoring: from qualitative to quantitative comparation," *Artificial Intelligence Review*, vol. 52, no. 1, pp. 217–243, 2019.

[9] G. Tang, K. Wu, and J. Lei, "A distributed and scalable approach to semi-intrusive load monitoring," *IEEE Transactions on Parallel and Distributed Systems*, vol. 27, no. 6, pp. 1553–1565, 2015.

[10] F. Xu, B. Huang, X. Cun, F. Wang, H. Yuan, L. L. Lai, and A. Vaccaro, "Classifier economics of semi-intrusive load monitoring," *International Journal of Electrical Power & Energy Systems*, vol. 103, pp. 224–232, 2018.

[11] G. Gagnon, S. Jomphe, D. Sicard, M. Dallaire, and D. Arbour, "Wireless sensor network for measurement of electrical energy consumption," Jan. 29 2019, uS Patent App. 10/191,095.

[12] A. L. Wang, B. X. Chen, C. G. Wang, and D. Hua, "Non-intrusive load monitoring algorithm based on features of v–i trajectory," *Electric Power Systems Research*, vol. 157, pp. 134–144, 2018.

[13] E. Aladesanmi and K. Folly, "Overview of non-intrusive load monitoring and identification techniques," *IFAC-PapersOnLine*, vol. 48, no. 30, pp. 415–420, 2015.

[14] Z. Erkin, J. R. Troncoso-Pastoriza, R. L. Lagendijk, and F. Pérez-González, "Privacy-preserving data aggregation in smart metering systems: An overview," *IEEE Signal Processing Magazine*, vol. 30, no. 2, pp. 75–86, 2013.

[15] G. W. Hart, "Nonintrusive appliance load monitoring," *Proceedings of the IEEE*, vol. 80, no. 12, pp. 1870–1891, 1992.

[16] J. Z. Kolter and T. Jaakkola, "Approximate inference in additive factorial hmms with application to energy disaggregation," in *Artificial intelligence and statistics*, 2012, pp. 1472–1482.

[17] T. Ji, L. Liu, T. Wang, W. Lin, M. Li, and Q. Wu, "Non-intrusive load monitoring using additive factorial approximate maximum a posteriori based on iterative fuzzy c-means," *IEEE Transactions on Smart Grid*, 2019.

[18] K. He, L. Stankovic, J. Liao, and V. Stankovic, "Non-intrusive load disaggregation using graph signal processing," *IEEE Transactions on Smart Grid*, vol. 9, no. 3, pp. 1739–1747, 2016.

[19] A. Faustine, N. H. Mvungi, S. Kaijage, and K. Michael, "A survey on non-intrusive load monitoring methodies and techniques for energy disaggregation problem," *CoRR*, vol. abs/1703.00785, 2017. [Online]. Available: http://arxiv.org/abs/1703.00785

[20] J. Kelly and W. Knottenbelt, "Neural nilm: Deep neural networks applied to energy disaggregation," in *Proceedings of the 2nd ACM International Conference on Embedded Systems for Energy-Efficient Built Environments*. ACM, 2015, pp. 55–64.

[21] R. Bonfigli, A. Felicetti, E. Principi, M. Fagiani, S. Squartini, and F. Piazza, "Denoising autoencoders for non-intrusive load monitoring: improvements and comparative evaluation," *Energy and Buildings*, vol. 158, pp. 1461–1474, 2018.

[22] T. Kato, H. S. Cho, D. Lee, T. Toyomura, and T. Yamazaki, "Appliance recognition from electric current signals for information-energy integrated network in home environments," in *International Conference on Smart Homes and Health Telematics*. Springer, 2009, pp. 150–157.

[23] L. De Baets, C. Develder, T. Dhaene, and D. Deschrijver, "Detection of unidentified appliances in non-intrusive load monitoring using siamese neural networks," *International Journal of Electrical Power & Energy Systems*, vol. 104, pp. 645–653, 2019.

[24] S.-Y. Lee, "Blind source separation and independent component analysis: A review," *Neural Information Processing-Letters and Reviews*, vol. 6, no. 1, pp. 1–57, 2005.

[25] S. Wold, K. Esbensen, and P. Geladi, "Principal component analysis," *Chemometrics and intelligent laboratory systems*, vol. 2, no. 1-3, pp. 37–52, 1987.

[26] L. Tong, V. Soon, Y.-F. Huang, and R. Liu, "Amuse: a new blind identification algorithm," in *IEEE international symposium on circuits and systems*. IEEE, 1990, pp. 1784–1787.

[27] A. Belouchrani, K. Abed-Meraim, J.-F. Cardoso, and E. Moulines, "A blind source separation technique using second-order statistics," *IEEE Transactions on signal processing*, vol. 45, no. 2, pp. 434–444, 1997.

[28] A. Yeredor, "Blind separation of gaussian sources via second-order statistics with asymptotically optimal weighting," *IEEE Signal Processing Letters*, vol. 7, no. 7, pp. 197–200, 2000.

[29] P. Comon, "Independent component analysis, a new concept?" *Signal processing*, vol. 36, no. 3, pp. 287–314, 1994.

[30] A. Hyvrinen and E. Oja, "Independent component analysis: algorithms and applications," *Neural Networks*, vol. 13, no. 4, pp. 411 – 430, 2000. [Online]. Available: http://www.sciencedirect.com/science/article/pii/S0893608000000265

[31] A. J. Bell and T. J. Sejnowski, "An information-maximization approach to blind separation and blind deconvolution," *Neural computation*, vol. 7, no. 6, pp. 1129–1159, 1995.

[32] E. G. Learned-Miller and W. F. John III, "Ica using spacings estimates of entropy," *Journal of machine learning research*, vol. 4, no. Dec, pp. 1271–1295, 2003.

[33] R. Boscolo, H. Pan, and V. P. Roychowdhury, "Independent component analysis based on nonparametric density estimation," *IEEE Transactions on Neural Networks*, vol. 15, no. 1, pp. 55–65, 2004.

[34] P. Tichavskỳ and Z. Koldovskỳ, "Fast and accurate methods of independent component analysis: A survey," *Kybernetika*, vol. 47, no. 3, pp. 426–438, 2011.

[35] P. Paatero and U. Tapper, "Positive matrix factorization: A non-negative factor model with optimal utilization of error estimates of data values," *Environmetrics*, vol. 5, no. 2, pp. 111–126, 1994.

[36] J. Bobin, J.-L. Starck, J. Fadili, and Y. Moudden, "Sparsity and morphological diversity in blind source separation," *IEEE Transactions on Image Processing*, vol. 16, no. 11, pp. 2662–2674, 2007.

[37] J. Bobin, J. Rapin, A. Larue, and J.-L. Starck, "Sparsity and adaptivity for the blind separation of partially correlated sources," *IEEE transactions on signal processing*, vol. 63, no. 5, pp. 1199–1213, 2015.

[38] P. Comon and C. Jutten, *Handbook of Blind Source Separation: Independent component analysis and applications*. Academic press, 2010.

[39] A. H. Sayed, *Fundamentals of adaptive filtering*. John Wiley & Sons, 2003.

[40] G. B. Samson, M.-A. Levasseur, F. Gagnon, and G. Gagnon, "Auto-calibration of hall effect sensors for home energy consumption monitoring," *Electronics Letters*, vol. 50, no. 5, pp. 403–405, 2014.

[41] A. Reinhardt, P. Baumann, D. Burgstahler, M. Hollick, H. Chonov, M. Werner, and R. Steinmetz, "On the accuracy of appliance identification based on distributed load metering data," in *2012 Sustainable Internet and ICT for Sustainability (SustainIT)*. IEEE, 2012, pp. 1–9.

Antoine Langevin received his BSc in Electrical Engineering from the École de Technologie Supérieure, Montreal in 2016. He then started graduate studies by joining the Synchromedia laboratory of the École de Technologie Supérieure. His current research project is on energy disaggregation using machine learning techniques. He also participates in the Smart ÉTS Residence project. His areas of interest in research are artificial intelligence, home/smart city, prototyping and embedded systems.

Ghyslain Gagnon received the Ph.D. degree in electrical engineering from Carleton University, Canada in 2008. He is now Dean of research and Professor at École de Technologie Supérieure, Montreal, Canada. He is a board member of ReSMiQ and was Director of research laboratory LACIME (2013-2020), a group of 15 faculties and nearly 150 highly dedicated students and researchers in microelectronics, digital signal processing and wireless communications. Highly inclined towards research partnerships with industry, his research aims at microelectronics, digital signal processing and machine learning with various applications, including health care, media art and building energy management.

Mohamed Cheriet received M.Sc. and Ph.D. degrees in Computer Science from the University of Pierre & Marie Curie (Paris VI) in 1985 and 1988 respectively. Since 1992, he has been a professor in the Automation Engineering department at the École de Technologie Supérieure (University of Quebec), Montreal, and was appointed full Professor there in 1998. Prof. Cheriet is the founder and director of Synchromedia which targets multimedia communication in telepresence applications. Dr. Cheriet research has extensive experience in cloud computing and network virtualization and softwarisation. In addition, Dr. Cheriet is an expert in Computational Intelligence, Pattern Recognition, Machine Learning, and Perception. Dr. Cheriet has published more than 450 technical papers in the field. He serves on the editorial boards of several renowned journals and international conferences. As Tier 1 Canada Research Chair on Sustainable and Smart Eco-Cloud, he leads the establishment of the first smart university campus in Canada, created as a hub for innovation and productivity at Montreal. Dr. Cheriet is a Fellow of the International Association of Pattern Recognition (IAPR), a Fellow of the Canadian Academy of Engineering (CAE), a Fellow of the Engineering Institute of Canada (EIC), a Fellow of Engineers Canada (EC), and the recipient of the 2016 IEEE J.M. Ham Outstanding Engineering Educator Award and of the 2012 Queen Elizabeth II Diamond Jubilee Medal. He is a senior member of the IEEE, the founder and former Chair of the IEEE Montreal Chapter of Computational Intelligent Systems (CIS), Steering Committee Member of the IEEE Green ICT Initiative, and Chair of IEEE ICT Emissions Working Group.